

The heavy quark potential and its mass dependence

A. Laschka, N. Kaiser and W. Weise

Physik Department, Technische Universität München, D-85747 Garching, Germany

Abstract. The heavy quark-antiquark potential is an important topic in QCD that involves perturbative as well as non-perturbative methods. We construct the perturbative short-distance part of the potential in coordinate space via a subtracted Fourier transform, covering the momentum region where perturbative QCD is applicable. This potential is matched at intermediate distances to the non-perturbative long distance part from lattice QCD simulations. In addition to the static potential, quark mass dependent contributions and their effects on the quarkonium spectrum are discussed. Furthermore we derive charm and bottom quark masses in this approach.

Keywords: QCD potential, Heavy quarks, Quarkonium spectrum

PACS: 12.38.-t, 12.39.Pn, 14.40.Pq, 14.65.Dw, 14.65.Fy

INTRODUCTION

The static potential between two infinitely heavy quarks is an object of interest since decades. Already a simple ‘‘Coulomb-plus-linear’’ shape is sufficient to understand roughly the observed quarkonium spectra. Nowadays the potential is defined in a non-relativistic effective theory framework. While the long distance part can be studied in lattice QCD simulations, perturbation theory should be expected to work at short distances.

Consider the perturbative static quark-antiquark potential at two-loop order in momentum space:

$$\tilde{V}^{(0)}(|\vec{q}|) = -\frac{16\pi\alpha_s(|\vec{q}|)}{3\vec{q}^2} \left\{ 1 + \frac{\alpha_s(|\vec{q}|)}{4\pi} a_1 + \left(\frac{\alpha_s(|\vec{q}|)}{4\pi} \right)^2 a_2 + \dots \right\}, \quad (1)$$

where \vec{q} is the three-momentum transfer. The constants a_1 and a_2 are [1, 2, 3]:

$$a_1 = 31/3 - 10/9 n_f, \\ a_2 = 456.749 - 66.3542 n_f + 1.23457 n_f^2,$$

where n_f is the number of light-quark flavors. Higher order terms have infrared contributions (e.g. [4]) and are not considered at this level. Expressing $\alpha_s(|\vec{q}|)$ in a power series expansion about α_s at a fixed scale μ leads to the standard definition of the r -space static potential,

$$V^{(0)}(r) = -\frac{4}{3} \frac{\alpha_s(\mu)}{r} \left\{ 1 + \frac{\alpha_s(\mu)}{4\pi} [a_1 + 2\beta_0 g_\mu(r)] + \left(\frac{\alpha_s(\mu)}{4\pi} \right)^2 [a_2 + \beta_0^2 (4g_\mu^2(r) + \pi^2/3) + 2g_\mu(r)(2a_1\beta_0 + \beta_1)] + \mathcal{O}(\alpha_s^3) \right\}, \quad (2)$$

with $g_\mu(r) = \ln(\mu r) + \gamma_E$. It is well known that this potential suffers from renormalon ambiguities [5, 6] and shows a badly convergent behavior [7].

STATIC AND ORDER 1/M POTENTIAL

We work in the following in the potential subtracted (PS) scheme proposed by Beneke [5] and use the alternative definition of the static r -space potential:

$$V^{(0)}(r, \mu_f) = \int_{|\vec{q}| > \mu_f} \frac{d^3q}{(2\pi)^3} e^{i\vec{q}\cdot\vec{r}} \tilde{V}^{(0)}(|\vec{q}|), \quad (3)$$

where $\tilde{V}^{(0)}(|\vec{q}|)$ is given in Eq. (1), but $\alpha_s(|\vec{q}|)$ is understood without resorting to a power series expansion. The momentum space cutoff μ_f is introduced in order to exclude the uncontrolled low momentum region.

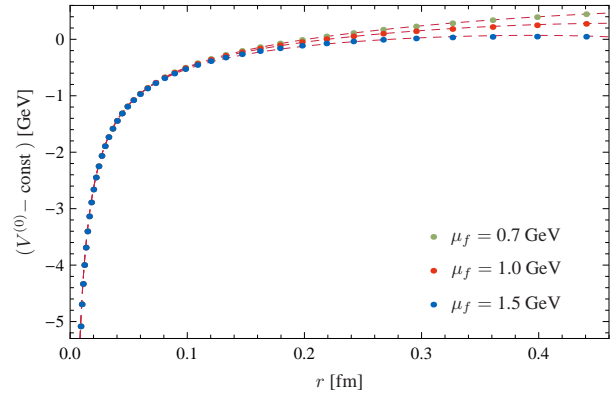


FIGURE 1. Static QCD potential (with $n_f = 3$) from the restricted numerical Fourier transform (3). The curves have been shifted by a constant to match at small r values.

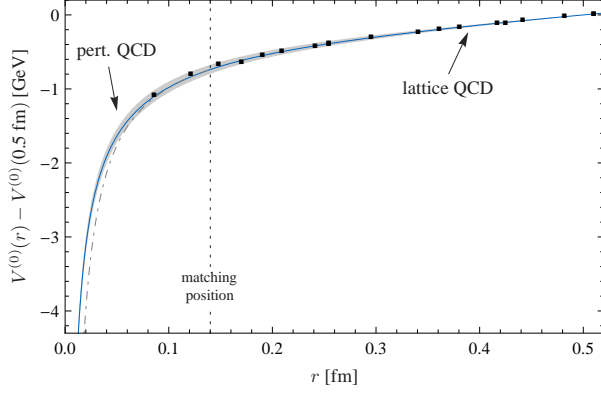


FIGURE 2. Static potential for $n_f = 3$, matched at $r = 0.14$ fm to a potential from lattice QCD [8].

The potential $V^{(0)}(r, \mu_f)$ is evaluated numerically using four-loop RGE running for the strong coupling α_s . For distances $r \lesssim 0.2$ fm, this potential depends only marginally on μ_f as shown in Fig. 1. The perturbative potential, valid at small distances, can be matched at intermediate distances to results from lattice QCD (see Fig. 2). As matching point (dashed line) we choose $r = 0.14$ fm where the perturbative and lattice potential are expected to be reliable. The gray band demonstrates uncertainties in the Sommer scale $r_0 = 0.50 \pm 0.03$ fm (lattice part) and in the scale dependence of $\alpha_s(|\vec{q}|)$ (perturbative part).

The overall constant of the static potential can be fixed by comparison with the masses of the experimentally measured quarkonium states. We find the values $m_{\text{PS}}(\mu_f = 0.908 \text{ GeV}) = 4.78 \text{ GeV}$ (bottomonium case) and $m_{\text{PS}}(\mu_f = 0.930 \text{ GeV}) = 1.39 \text{ GeV}$ (charmonium case). The potential subtracted (PS) quark mass can be converted to the $\overline{\text{MS}}$ mass. The corresponding analytic formula is less reliable for $\mu_f \approx 0.9 \text{ GeV}$ than for μ_f close to the heavy quark mass. Therefore it is favorable to use (instead of matching at point (1) in Fig. 3) the numerical μ_f dependence first to translate $m_{\text{PS}}(\mu_f)$ into $m_{\text{PS}}(\bar{m})$ and afterwards translate this value into the $\overline{\text{MS}}$ scheme (corresponding to point (2)). By this method the extraction of \bar{m} becomes independent of the value of μ_f that we use in the construction of our potential. This leads in our model to the quark masses: $\bar{m}_b = 4.20 \text{ GeV}$ for the bottom quark and $\bar{m}_c = 1.23 \text{ GeV}$ for the charm quark in the $\overline{\text{MS}}$ scheme.

The heavy quark-antiquark potential can be written in a power series of the inverse quark mass m :

$$V(r) = V^{(0)}(r) + \frac{V^{(1)}(r)}{m/2} + \frac{V^{(2)}(r)}{(m/2)^2} + \dots \quad (4)$$

$V^{(1)}$ is spin independent and the first mass dependent correction to the static potential. It reads in momentum

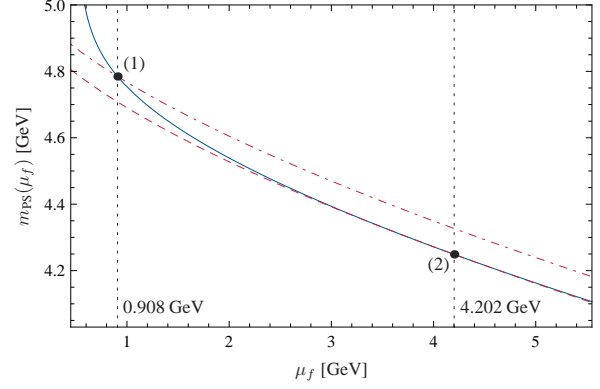


FIGURE 3. Scale dependence of $m_{\text{PS}}(\mu_f)$. The solid curve shows the numerical μ_f dependence, the dashed and dot-dashed curves show the analytical μ_f dependence. For the determination of \bar{m}_b matching at point (2) is preferred.

space:

$$\tilde{V}^{(1)}(|\vec{q}|) = -\frac{2\pi^2 \alpha_s^2(|\vec{q}|)}{|\vec{q}|} \{1 + \mathcal{O}(\alpha_s)\}, \quad (5)$$

and can be transformed analogously as in Eq. (3) to position space (with a low momentum cutoff μ'_f). At long distances $V^{(1)}(r)$ is known from lattice QCD [9, 10]. To fit the lattice data we use the form

$$V_{\text{fit}}^{(1)}(r) = -\frac{c'}{r^2} + d' \ln r + \text{const}, \quad (6)$$

motivated in [11]. As shown in Fig. 4 matching with the perturbative potential at intermediate distances is also possible at order $1/m$.

To obtain values for the quark masses at this order a redefinition of the PS mass is needed

$$m_{\widehat{\text{PS}}}(\mu_f, \mu'_f) \equiv m_{\text{PS}}(\mu_f) - \frac{1}{2m} \alpha_s^2(\bar{m}) \mu_f^2. \quad (7)$$

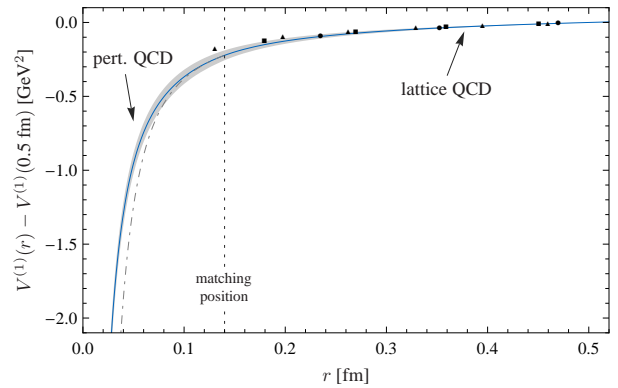


FIGURE 4. The order $1/m$ potential with $n_f = 3$, matched at intermediate distances in coordinate space to a potential from lattice QCD.

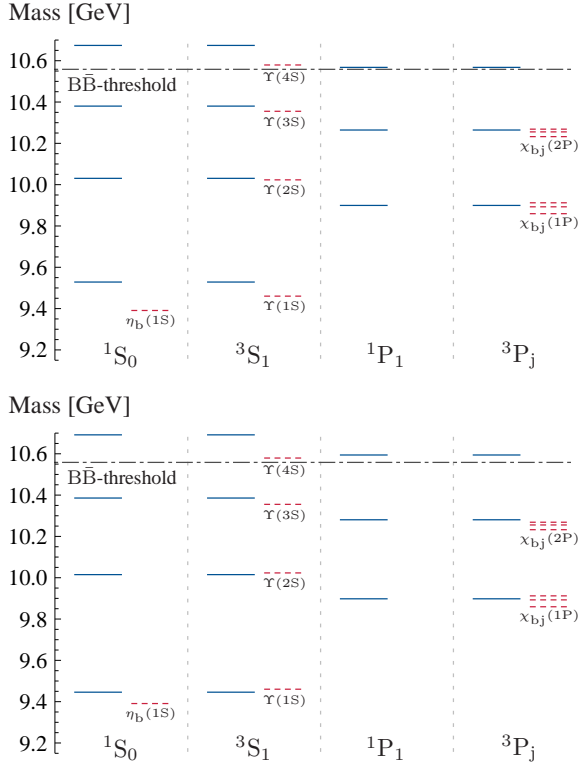


FIGURE 5. Bottomonium spectrum. In the upper plot the potential $V^{(0)}$ is used, in the lower plot $V^{(0)} + \frac{V^{(1)}}{m/2}$. Dashed lines show measured states, solid lines are model predictions.

This leads to the heavy quark masses listed in the following table and compared to values given by the Particle Data Group [12].

	\overline{MS} masses [GeV]		
	static	static + $\mathcal{O}(1/m)$	PDG 2010
bottom quark	4.20	4.18	$4.19^{+0.18}_{-0.06}$
charm quark	1.23	1.28	$1.27^{+0.07}_{-0.09}$

SPECTROSCOPY

Quarkonium spectra can be deduced (Fig. 5 and Fig. 6) from the potentials we constructed in the previous sections. They are shown with and without order $1/m$ effects. Note that the only free parameter is the heavy quark mass which is chosen such as to reproduce the 1^3P_1 -state. Spin dependency is not treated yet, since it is an order $1/m^2$ effect. The next step is to systematically include $1/m^2$ terms. They are expected to be sizeable, especially in the case of charmonium. A more detailed presentation is found in [13].

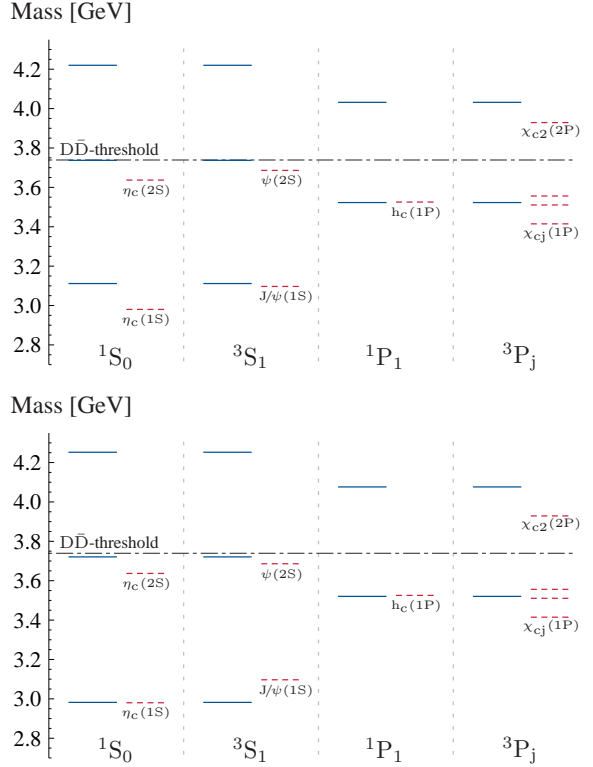


FIGURE 6. Charmonium spectrum. In the upper plot the potential $V^{(0)}$ is used, in the lower plot $V^{(0)} + \frac{V^{(1)}}{m/2}$. Dashed lines show measured states, solid lines are model predictions.

ACKNOWLEDGMENTS

Work supported in part by BMBF, GSI and the DFG Excellence Cluster “Origin and Structure of the Universe”.

REFERENCES

1. M. Peter, *Phys. Rev. Lett.* **78**, 602–605 (1997).
2. M. Peter, *Nucl. Phys.* **B501**, 471–494 (1997).
3. Y. Schröder, *Phys. Lett.* **B447**, 321–326 (1999).
4. N. Brambilla, A. Pineda, J. Soto, and A. Vairo, *Phys. Rev.* **D60**, 091502 (1999).
5. M. Beneke, *Phys. Lett.* **B434**, 115–125 (1998).
6. A. H. Hoang, et al., *Phys. Rev.* **D59**, 114014 (1999).
7. A. Pineda, *J. Phys.* **G29**, 371–385 (2003).
8. G. S. Bali, et al., *Phys. Rev.* **D62**, 054503 (2000).
9. Y. Koma, M. Koma, and H. Wittig, *Phys. Rev. Lett.* **97**, 122003 (2006).
10. M. Koma, Y. Koma, and H. Wittig, *PoS Confinement8*, 105 (2008).
11. G. Perez-Nadal, and J. Soto, *Phys. Rev.* **D79**, 114002 (2009).
12. K. Nakamura, et al., *J. Phys.* **G37**, 075021 (2010).
13. A. Laschka, N. Kaiser, and W. Weise, *preprint* (2010).